Reshaping of Freely Propagating Terahertz Pulses by Diffraction

Ajay Nahata and Tony F. Heinz

Abstract—We discuss the application of diffraction theory to the reshaping of freely propagating terahertz pulses by narrow apertures. This is accomplished by using two separate electrooptic sampling detectors. The first contains a narrow electrode geometry that does not modify the frequency content of the incident terahertz field, while the second contains a narrow gap between two large electrodes. The latter detector transforms the incident bipolar terahertz waveform into a unipolar waveform. We find that diffraction theory properly accounts for this reshaping process. We discuss the applicability of alternate electrode geometries for terahertz pulse shaping.

I. INTRODUCTION

DIFFRACTION of electromagnetic radiation through apertures has been the subject of intense research over the last century [1], [2] and remains a topic of great interest and importance. In the field of terahertz (THz) optoelectronics, apertures are routinely encountered in a number of different elements and have been shown to alter the temporal properties of the freely propagating THz radiation. These apertures may be formed, for example, by the electrodes of photoconductive detectors and emitters [3]. Circular apertures also frequently occur in THz systems, such as in the use of hyperhemispherical lenses [4], [5]. Further, several investigators noted that apertures in the propagation path of the THz beam can alter the electric field envelope of the pulse [6]–[8].

A classic problem in diffraction theory, first examined by Rayleigh [1], concerns the effect of a narrow slit in a two-dimensional screen on incident electromagnetic radiation. This geometry occurs commonly in devices employed throughout the electromagnetic spectrum and has also been exploited in experiments involving broad-band THz radiation generated by ultrafast laser pulses. In the latter case, we wish to understand how the *spectral content* and *temporal characteristics* of broad-band pulses are altered, in addition to considering the traditional issue of how the spatial distribution of the incident radiation is perturbed by diffracting elements. Given the large fractional bandwidth of THz radiation generated by ultrafast laser pulses, the influence of diffraction on the temporal characteristics of a pulse can be significant. For example, in early experiments concerning the detection of freely propagating THz radiation, Auston and coworkers employed a

geometry in which a photoconductive medium was placed in a narrow gap between conducting electrodes [3]. The researchers found that the electrodes transformed the shape of the electromagnetic transient being detected. Rather than the expected bipolar shape for the time evolution of the electric field, the experimental data revealed a unipolar waveform. This effect was ascribed to the influence of diffraction and was modeled by a simple integration in time of the waveform. A similar type of phenomenon was also observed by van Exter and Grischkowsky [9]. These authors compared the THz field measured by a Hertzian dipole antenna and a simple gap detector and demonstrated clearly the enhanced high-frequency response of the former detector relative to the latter detector.

In recent investigations in our laboratory, we also observed significant reshaping of freely propagating THz pulses in our detector structures. In these measurements, we employed electrooptic sampling with the active medium embedded within a narrow gap between two large-area electrodes (LAE) that were used as poling electrodes [10]. The observed THz waveform was again found to be unipolar, rather than the expected bipolar shape. We attributed the reshaping of the incident THz pulse to diffraction induced by the metal electrodes. To study this effect further, we compared the measured THz waveform with that obtained with a photoconductive dipole detector. In keeping with the earlier treatment of [3], we applied a simple integration of the signal from the dipole detector to model the effect of diffraction present in the electrooptic sampling element. This method of analysis yielded results that were qualitatively similar to our observations. However, since the photoconductive detector imposed an additional system response function on the measured THz field, the procedure was not suitable for quantitative comparison.

It is the aim of the present publication to provide quantitative study of the influence of diffraction on a pulse of THz radiation incident on a narrow slit in a conducting screen. The role of diffraction is examined by considering the perturbed electromagnetic field present in the plane of the screen. From an experimental point of view, we have addressed this issue using the techniques of coherent THz spectroscopy with electrooptic sampling of the THz waveform. In this approach, an ultrafast THz electromagnetic transient is first generated by a femtosecond laser pulse. The freely propagating THz radiation is then detected by electrooptic sampling in a thin film of nonlinear material, permitting us to obtain an accurate measurement of the electric field waveform. To probe the effects of diffraction, we have per-

formed measurements with two different detection geometries. In one case, the electrooptic sampling occurs within the gap of two large electrodes, allowing us to observe the strongly diffracted field. To calibrate this measurement, one would ideally eliminate the electrodes. However, in practice, these electrodes could not be removed because of the fabrication procedure. Consequently, for the second geometry, we used an electrooptic sampling element (EOSE) having only thin metal lines to characterize the THz waveform. As discussed below, we find that diffraction effects in this latter structure do not alter the shape of the THz waveform appreciably. Thus, we have a reference waveform with which to calibrate the strongly perturbed waveform present in the gap of the large area electrodes. The experimental studies were conducted with the THz radiation incident on the screen at normal incidence and with the THz electric field polarized perpendicular to the gap.

The analysis of the influence of diffraction on the THz waveform developed in this paper is based on the application of rigorous diffraction theory for radiation impinging on a narrow gap in a perfectly conducting screen. We demonstrate that application of diffraction theory yields a transformation of the incident THz waveform as it propagates into the gap, which while similar to the simple integration model previously employed, gives rise to readily discernible differences in the predicted waveforms. In particular, the rigorous calculation indicates that the high frequency components are less strongly suppressed than in the integration model. Given the improved experimental data reported here, we can confirm the improved accuracy of the model based on diffraction theory compared with the simple integration scheme. An important aspect of the current measurements is the coherent nature of the detection technique. Since the electric field is measured, both the amplitude and phase may be obtained. Therefore, we may ascertain the effects of the amplitude and phase functions, related to the diffraction process, on the measured waveform. From the point of view of diffraction theory, we may also note that these measurements probe the influence of diffraction on the near fields, rather than on the re-radiated fields frequently measured in the optical part of the spectrum. In addition to the case of an electric field polarized perpendicular to the gap, we present calculations for the case of the electric-field polarized along the axis of the gap. This case is found to give rise to a completely different reshaping of the spectral content of the incident pulse. These results suggest the possibility of controlled reshaping of THz waveforms using diffractive structures, a subject that we discuss briefly. In recent studies by Bromage *et al.* [11], several interesting possibilities have been examined both experimentally and theoretically.

II. DIFFRACTION MODEL

We have developed a model that describes the reshaping of the THz pulse by the large area electrodes (LAE) that is based on the classical electromagnetic problem of diffraction by a two-dimensional (2-D) screen with a narrow slit. To compare predictions of this model with experiment, we must be able to measure accurately the incident THz electric field. As indicated
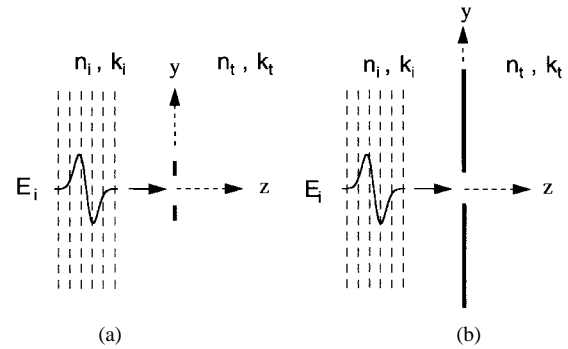

Fig. 1. (a) Diffraction of a plane electromagnetic plane wave by a narrow coplanar electrodes embedded in a homogeneous medium. (b) Diffraction of a plane electromagnetic plane wave by a 2-D screen with a narrow slit. Different homogeneous media are present on either side of the electrodes. In the experiments, the incident electric field is polarized perpendicular to the gap.

in the introduction, we have employed a narrow electrode geometry to obtain this reference waveform. We must, therefore, first determine the effect of the narrow electrode strips on the incident THz field. The experimental geometry is shown in Fig. 1(a). For simplicity, we consider the effect of a single, infinitely thin, perfectly conducting metal strip, of width $2a$, in a homogeneous medium with a THz refractive index n (assumed to be lossless and frequency independent). The origin of the y-axis for the single strip is located at the center of the strip. The normally incident plane wave electric field, E_i, is polarized perpendicular to the strip. An iterative solution has been developed [12], [13] for the scattered electric field on the portions of the $z = 0$ plane (y-axis) not occupied by the strip. We consider here the response for each frequency ω with wavevector $k = n\omega/c$. For $ka \ll 1$, we may use the first-order solution for the scattered field, E_{sc}, which is expressed as [12], [13]

$$\frac{E_{sc}(y)}{E_i}\bigg|_{z=0} \cong \frac{\exp\left[i2ky\right]}{\pi\sqrt{\left(\frac{y}{a}\right) - 1}} \int_{-1}^{1} \frac{\exp\left[\frac{ika\rho}{4}\right]\sqrt{\rho + 1}}{\left(\frac{y}{a}\right) + \rho}\, d\rho$$

$$\text{(valid for } y \geq a). \tag{1}$$

An equivalent expression may be written for $y \leq -a$. In our experimental geometry, we used 10-μm-wide ($=2a$) electrode strips. Using this value, and assuming a refractive index of $n = 2$, we have calculated the relative scattered electric field as a function of distance from the strip edge and as a function of frequency. We have found that, while the perturbation can be significant near the strip edge, it is nearly frequency independent for all distances from the metal strip (again, for $k \ll 1/a$). Scattering of an incident electric field caused by a pair of strip electrodes in close proximity to one another has not, to our knowledge, been solved. However, based on the single electrode results, we believe that the perturbation to the electric field between the electrodes will remain frequency independent. This assumption is consistent with our experimental results, as discussed below. It can also be reasoned on general grounds, since we may approximate the near-field diffraction problem occurring in structures with

all (relevant) dimensions $d \ll 1/k$ using an electrostatic analysis. Thus the modification of the field by diffraction will be frequency independent. In short, we conclude that the THz field measured with the narrow electrode geometry detector is directly proportional to the incident electric field.

We now turn to our diffracting electrode geometry. This experimental geometry is shown schematically in Fig. 1(b). The THz field, which is incident from the left onto the conducting screen at normal incidence, is diffracted into the medium on the right. The gap runs along the x-axis and has a width of $2b$. Different homogeneous media are present on either side of the conducting screen, where the subscripts i and t denote the medium of incidence and medium of transmission, respectively. Each medium is characterized by a THz refractive index n (again assumed to be lossless and frequency independent).

The narrow slit diffraction problem was first examined by Rayleigh [1] and has been the subject of great attention ever since [2]. Here, we are concerned with the case of the screen separating two distinct homogeneous media. The general formulation of this problem leads to complex integro-differential equations. However, in the limit of a narrow gap, one may obtain an analytic solution to the problem as a series expansion in powers $k_i b$, as shown by Houlberg [14]. We find that for the frequency range considered in this study, the leading-order term in powers of $k_i b$ is adequate for our purposes. We denote by $E_{ap}(\omega)$, the electric field present in the gap due to a monochromatic plane wave and by $E_i(\omega)$, the electric field approaching the screen at normal incidence. The incident field, and therefore the aperture field, is assumed to be polarized perpendicular to the gap, i.e., along the y-axis in Fig. 1(b). From Houlberg's result, it can be shown that the relative aperture field, to first order, is given by [14]

$$\frac{E_{ap}^y(y, z=0)}{E_i(y, z=0)} = \frac{-i}{k_i b} \frac{2}{p_o}\left[1 - \frac{y^2}{b^2}\right]^{-1/2} \quad (2)$$

where

$$p_o = 2\ln(\gamma) + 2\ln\left(\frac{k_i b}{4}\right) - i\pi + 2\ln\left(\frac{n_t}{n_i}\right). \quad (3)$$

In this expression, $\gamma(=1.781\cdots)$ is Euler's constant, and $k_i = n_i \omega/c$ is the wavevector in incident medium for radiation of frequency ω. A higher order solution for the aperture field is given in the Appendix.

In general, an accurate description of the sampled field in the electrode gap requires the use of an overlap integral involving the aperture field and the probe beam. However, examination of (2) shows that the frequency content of E_{ap} is spatially invariant. Therefore, the frequency dependence of the sampled aperture field, E_{samp}, may be found from the aperture field E_{ap} evaluated anywhere in the gap. As an estimate of the typical magnitude of the sampled field, we may take, for example, a uniform spatial average over the gap. This approach yields

$$E_{samp}(\omega) = \frac{1}{2b}\int_{-b}^{b} E_{ap}^y(y, z=0) \cdot dy$$
$$= \frac{-i\pi}{k_i b}\frac{1}{p_o} E_i(\omega). \quad (4)$$

The exact treatment of the spatial sampling, it should be stressed, does not alter the predicted temporal characteristics of the measured waveform. At this level of approximation, only the magnitude of the sampled field is affected.

A similar type of expansion may be used to estimate the aperture field in the case where the incident monochromatic plane wave, $E_i(\omega)$, is polarized *parallel* to the gap. In this case, the incident field, and therefore the aperture field, is polarized along the x-axis. While we have not considered this case experimentally, this geometry could be examined by applying electrodes to an electrooptic sampling element in the appropriate orientation. This observation highlights an important distinction between electrooptic sampling and photoconductive sampling: the latter technique can not be used for this configuration since no current would flow between the electrodes. The relative aperture field for this geometry is given by [14]

$$\frac{E_{ap}^x(y, z=0)}{E_i(y, z=0)} = -ik_i b\left[1 - \frac{y^2}{b^2}\right]^{1/2}. \quad (5)$$

We may again define an average aperture field, as we did in (4), to yield

$$E_{samp}(\omega) = \frac{1}{2b}\int_{-b}^{b} E_{ap}^x(y, z=0) \cdot dy$$
$$= \frac{-i\pi k_i b}{4} E_i(\omega). \quad (6)$$

A higher order solution for the aperture field in this geometry is given in the Appendix.

The dielectric properties used in this model are those of sapphire ($n_i = 3.1$) [15] and air ($n_t = 1$). The slit width ($=2b$) is 25 μm in the measurements and simulations. The amplitude and phase functions obtained from evaluating (4) and (6) as a function of THz frequency are shown in Figs. 2(a) and 3(a), respectively. An interesting situation arises for the case of incident electric field E_i polarized perpendicular to the gap. In this case, we see that the magnitude of the diffracted electric field in the gap of the narrow aperture may significantly exceed that of the incident field at low frequencies. This is in sharp contrast to the case when the electric field is polarized parallel to the gap. Here, the low-frequency components of the diffracted field in the gap are severely reduced in amplitude (high-pass filter). This behavior simply reflects the fact that the boundary condition causes the electric field parallel to the gap to vanish at the edge of the metal, while a perpendicular electric field may be sustained at the boundary. Further, the temporal waveform of the diffracted field is proportional to the first derivative of the incident field. This is exemplified by using an idealized bipolar function [top trace in Fig. 3(b)] as the form of the incident electric field. The resulting (normalized) diffracted electric field is shown in the lower trace in Fig. 3(b).

III. EXPERIMENTAL ARRANGEMENT AND ELECTROOPTIC SAMPLING MEASUREMENTS

We fabricated EOSE's, shown schematically in Fig. 4(a), on c-cut sapphire substrates. High-reflectivity dielectric coatings
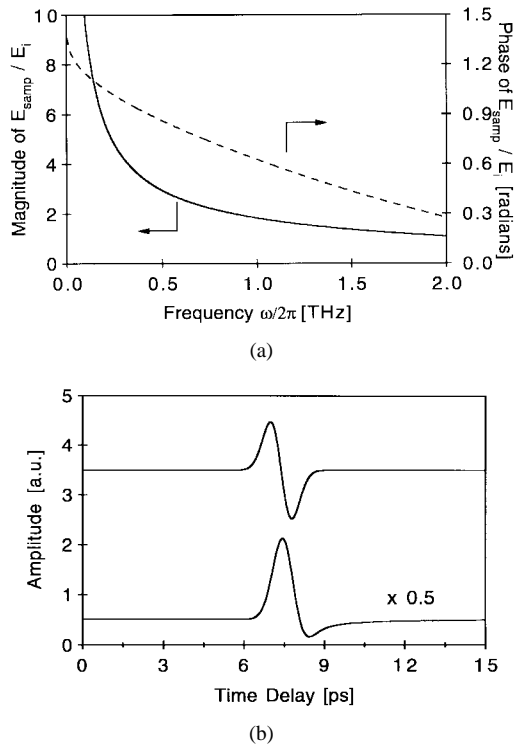
(a)

(b)

Fig. 2. (a) Amplitude (solid curve) and phase (dashed curve) spectrum of $E_{\mathrm{samp}}(\omega)/E_i(\omega)$ for the case where the incident electric field is polarized perpendicular to the gap. (b) An idealized bipolar waveform (top trace) is used to simulate the effect of this electrode geometry. The resulting diffracted field (lower trace) is unipolar and has a peak-to-peak value that is approximately a factor of 2 larger the incident field.

(a)

(b)

Fig. 3. (a) Amplitude (solid curve) and phase (dashed curve) spectrum of $E_{\mathrm{samp}}(\omega)/E_i(\omega)$ for the case where the incident electric field is polarized parallel to the gap. (b) An idealized bipolar waveform (top trace) is used to simulate the effect of this electrode geometry. The resulting diffracted field (lower trace) is directly proportional to the first derivative of the incident field and has a peak-to-peak value that is approximately a factor of 5 smaller the incident field.

centered at 800 nm were evaporated onto one side of the sapphire substrate to permit the sampling to be performed in a reflection geometry. Different electrode structures were then photolithographically defined on the substrates. These geometries consisted of: a) 5-mm-long × 10-mm-wide electrodes separated by 25 μm (LAE), b) 10-mm-long × 10-μm-wide electrodes separated by 25 μm ("10–25–10"), and c) 10-mm-long × 10-μm-wide electrodes separated by 10 μm ("10–10–10"). The first electrode geometry is shown on the left in Fig. 4(b), while the latter two electrode geometries are depicted on the right in Fig. 4(b). A nonlinear optical polymer film [16], nominally 10-μm thick, was solution cast onto each substrate and poled at the glass transition temperature of the polymer. A high-resistivity silicon hyper-hemispherical lens was attached to each device to focus the THz radiation into the electrode gap region.

The experimental setup for generating and detecting THz radiation is shown in Fig. 4(c). A 76 MHz mode-locked Ti : sapphire laser operating at 800 nm was used to generate and detect the transient THz pulses. A collimated 2-mm-diameter pump beam, with average power of 400 mW, served to drive a large aperture photoconducting emitter. The emitter was oriented so that the resulting THz electric field was parallel to the c-axis of the poled polymer and perpendicular to the edges of the electrode structures. Two off-axis paraboloidal mirrors were used to collimate and focus the THz radiation into the EOSE. The total separation between the emitter and detector was 60 cm.
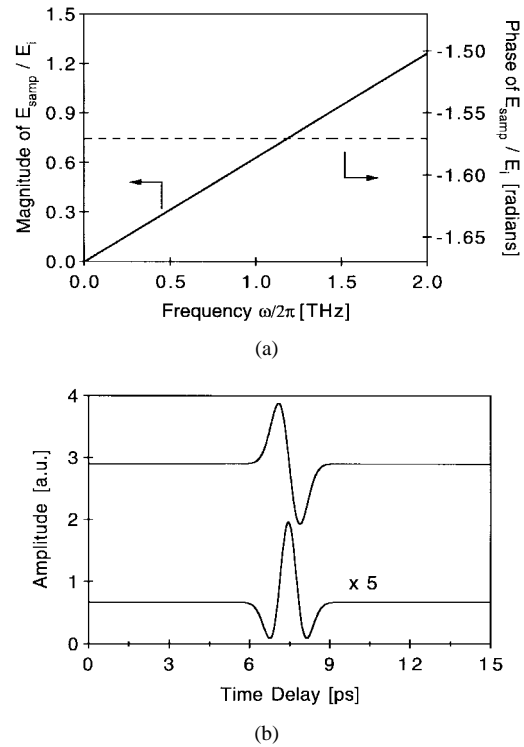
The detection system employed a crossed polarizer arrangement with differential detection [17]. The probe beam was optically biased at its quarter wave point by a Soleil–Babinet compensator and focused into the electrode gap of the EOSE, so that it made a double pass through the polymer film. The reflected probe beam was split by the Wollaston prism and generated a quiescent current of approximately 1 mA in each photodetector. The differential signal was amplified, digitized, and averaged using a computerized data acquisition system.

The temporal waveform of the THz electric field measured by electrooptic sampling with the LAE device is shown in Fig. 5(a). As with our earlier work, the observed waveform is unipolar, suggesting strong perturbation of the incident THz radiation induced by diffraction from the electrodes. The amplitude spectrum for the experimental waveform of Fig. 5(a) is shown in Fig. 6(a). We also measured the THz electric field using both the 10–25–10 and 10–10–10 devices. The temporal waveform obtained with the 10–25–10 device is depicted in Fig. 5(b) and the corresponding amplitude spectrum is displayed in Fig. 6(b). The temporal waveforms from the 10–25–10 structure and 10–10–10 structure (not shown) were found to be identical within experimental accuracy. This behavior confirms the conclusion drawn from analysis of (1) that the narrow-strip electrodes do not modify the frequency content of the incident field. Thus, in the analysis discussed below, we treat the measurements from the 10–25–10 devices as representing the true incident THz waveform.
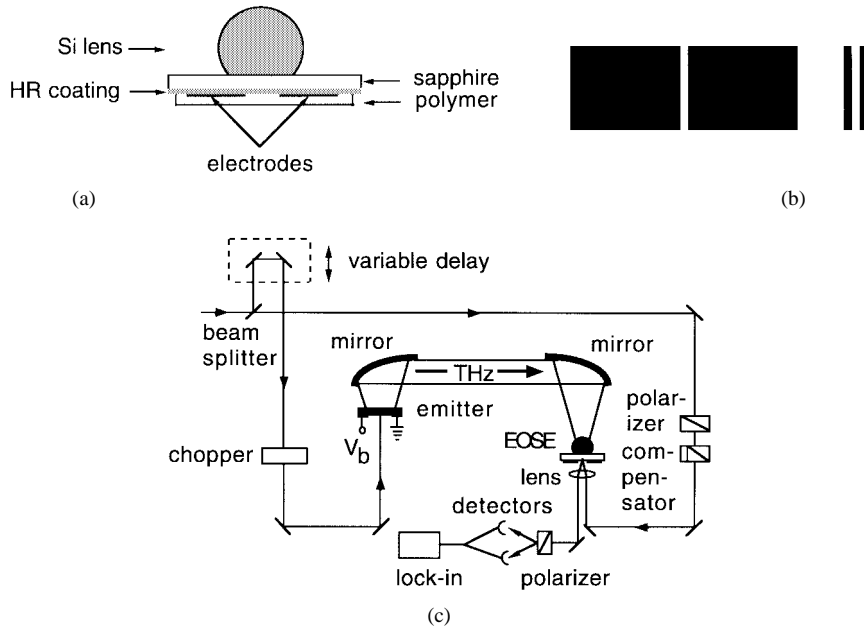
Fig. 4. (a) Schematic drawing of the electrooptic sampling element. (b) Schematic representation of the large area electrodes (left) and the narrow electrode geometry (right). (c) Schematic drawing of the experimental setup used to generate and detect freely propagating THz radiation.
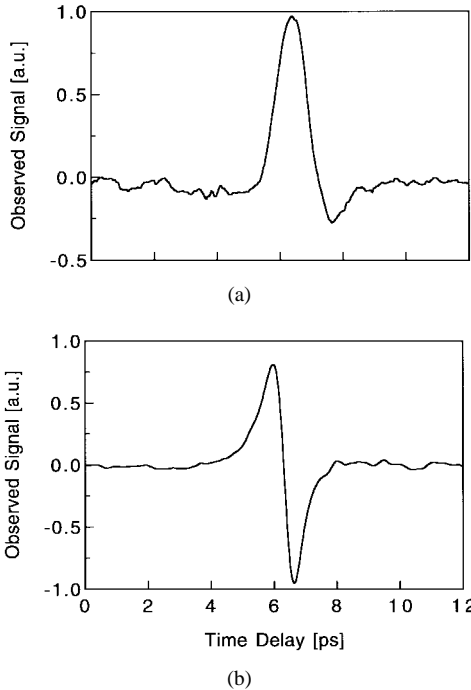

Fig. 5. Temporal waveform measured with the (a) LAE device and (b) 10–25–10 device. A large aperture antenna was used as the emitter.
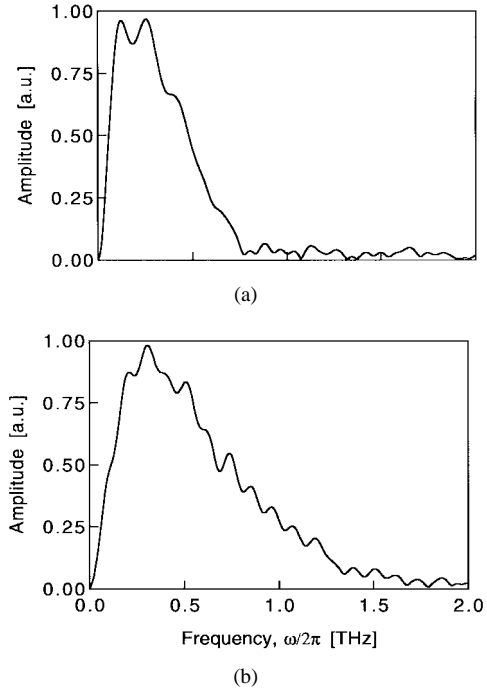

Fig. 6. Amplitude spectrum obtained from (a) the LAE device [Fig. 5(a)] and (b) 10–25–10 device [Fig. 5(b)].

IV. APPLICATION OF DIFFRACTION THEORY AND DISCUSSION

As stated earlier, all experimental parameters, aside from the electrode geometry, were the same for the two (LAE and 10–25–10) detector structures. Consequently, parameters such as the optical pulsewidth, the roundtrip transit time, the material response time, the THz absorption in the device, etc. enter into both measurements in an equivalent fashion. We may, therefore, apply the diffraction result embodied in (4) taking the waveform measured by the 10–25–10 device as the incident field, $E_i(\omega)$, without any further consideration of the system response.

It is worth examining the differences between the present diffraction transfer function and that obtained from a simple integration [$i\omega^{-1}E_i(\omega)$]. The primary difference may be seen by comparing the frequency dependence of the transfer functions E_{samp}/E_i, presented in Fig. 7, in each calculation. The transfer function for the integration model suppresses the high-frequency components more strongly than the diffraction calculation of (4). The difference is primarily the result of an
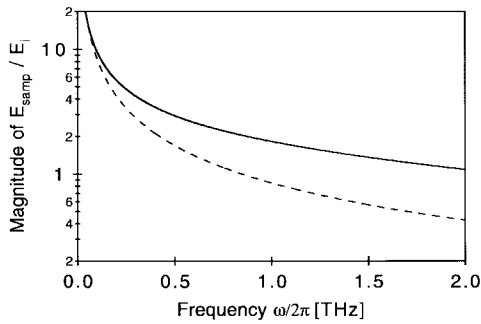
Fig. 7.	Amplitude spectrum of the relative aperture field using the diffraction model of (4) (solid curve) and the simple integration model (dashed curve). The incident electric field is polarized perpendicular to the gap.
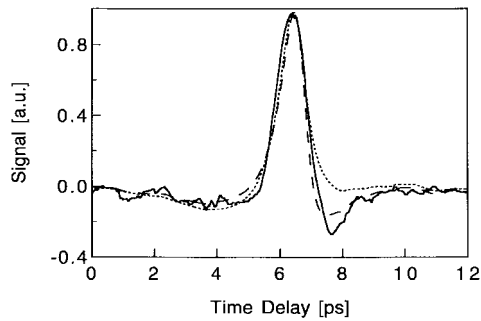

Fig. 8.	Simulation of the effects of diffraction using the frequency response of the 10–25–10 device [Fig. 6(b)] as the form of the incident field. The incident waveform is spectrally filtered using (4), then transformed back to the time domain (long dashed trace). For comparison, the experimentally measured unipolar waveform is shown [from Fig. 5(a)—solid trace], as well as the effect of using the simple integration model (short dashed trace).

additional factor with a logarithmic frequency dependence in the transfer function for the diffraction calculation. Also the phase of the transfer function corresponding to (4) is strongly frequency dependent, in contrast to the constant $\pi/2$ phase shift associated with the integration model.

The effects of diffraction for the experimental data have been simulated by taking the spectrum of the sampled waveform from the 10–25–10 structure as $E_i(\omega)$ [Fig. 6(b)] and then calculating the spectrum of the diffracted field from (4). The reshaped spectrum was numerically transformed to the time domain. The computed temporal response is shown in Fig. 8. For comparison, we also display the experimental data from the LAE device [Fig. 5(a)] and the results obtained from the integration model. We see that the predictions of (4) are in good general agreement with the experimental results and provide a significantly better fit than the integration model. We note that negative peak after the main pulse predicted in the diffraction calculation is somewhat less pronounced than in the experimental data. Simulations suggest that this discrepancy may be due to the changes in the ambient water vapor in the THz beam line (relative humidity of the laboratory) during the course of the experiments [18].

While the diffraction model presented provided reasonably good agreement with the experimental results, it is worthwhile to point out some of the approximations involved in its application. First, the analytic solution employed represents a leading-order approximation valid in the limit of the aperture

being much narrower than the THz wavelengths involved ($b \ll 1/k$). We believe that the solution used represents an adequate approximation for our purposes, since inclusion of higher-order terms in kb (from the relations given in the appendix) did not significantly alter the predicted waveforms. Second, the diffraction problem considered involved two homogeneous media. In fact, we had a thin (10 μm) film of the electrooptic polymer between the substrate and the top of the detector. However, since the thickness of this film is much less than the relevant THz wavelengths, we do not expect it to alter the frequency dependence of the diffraction process. Moreover, in the approximation of a leading order solution to the diffraction problem [as embodied in (4)], there is only a minor dependence on the value of the refractive index in the medium lying beyond the aperture. This result (only valid to leading-order in kb) further supports the notion of insensitivity to the presence of a thin film near the plane of the aperture. Another approximation implicit in the diffraction calculation involves the assumption of perfectly conducting metal electrodes. We believe that this is a reasonable approximation, since the anticipated dissipation in the metallic films over the scale of a THz wavelength is modest. A final simplification in the model is the treatment of the incident THz field as a plane wave. Experimentally, this is not the case, since the radiation is focused into the gap for enhanced detection sensitivity. The influence of this bending of the wavefronts is expected to be relatively modest, however, in the limit of a narrow gap relevant to our experiment. Further measurements and calculations would be required to assess which of these factors might be of the greatest importance for further refinement of the model.

V. Conclusion

We have used a model based on diffraction by a narrow slit to account for the unipolar waveform obtained using an electrooptic sampling element containing large area electrodes with a narrow electrode gap, when irradiated by an incident THz field with a bipolar temporal evolution. This was accomplished by comparing waveforms obtained with a sampling element containing electrodes that did not modify the frequency content of the incident THz field. The good agreement between the experimental results and the model suggests diffraction alone accounts for the complete reshaping process. Aside from the dramatic reshaping process, this electrode configuration also exhibits the interesting characteristic of amplifying the peak THz field in the gap. We have also analyzed the diffractive properties of the electrode configuration where the incident THz field is polarized parallel to the aperture. In this geometry, the low frequency components of the incident field are strongly suppressed and the diffracted waveform is proportional to the first derivative of the incident field. Thus, the results also suggest that it may be possible to shape THz pulses using variously configured apertures in conducting screens.

Appendix

The section gives the higher order expansion for the electric field in a narrow aperture in powers of kb, where $2b$ is the

slit width. We assume an incident plane-wave electric field at normal incidence. The equations follow from the development by Houlberg [14]. Related treatments have also been given by Bouwkamp [2], Millar [19], and Butler and co-workers [20], [21]. These higher order corrections become more significant with increasing frequency for a fixed experimental geometry or with increasing gap spacing for a given range of frequencies.

For reference, in our experimental geometry with the electric field perpendicular to the gap, $k_i b = 0.4$ at a frequency of 0.5 THz. In the lowest order approximation, E_{ap}/E_i (evaluated at $y = 0$) $= 1.86$. The next higher order contribution $\Delta[E_{ap}/E_i](y = 0) = 0.16$. It is important to note that this higher order correction is largest at $y = 0$ and plays a more significant role at higher frequencies.

A. Electric Field Polarized Perpendicular to the Aperture

We begin by considering the case where the incident electric field is y-polarized. A schematic drawing of the problem is shown in Fig. 1(b). The relative aperture field is given by

$$\frac{E_{ap}^y(y, z = 0)}{E_i(y, z = 0)} = \frac{-i}{k_i b}\left[1 - \frac{y^2}{b^2}\right]^{-1/2}\sum_{j=0}^{\infty} C_j \cos(jv) \quad \text{(A1)}$$

where C_j are expansion coefficients and $\cos(v) = y/b$. The first three nonzero expansion coefficients are

$$C_0 = \frac{2}{p_o} + \frac{1}{4}\frac{p_2}{p_o^2}(k_i b)^2 + \left[\frac{1}{128}(-9p_4 + 3m_4)\right.$$
$$\left. -\frac{1}{32m_o}\left(p_2 + \frac{m_2}{2}\right)^2 + \frac{1}{8}\frac{p_2^2}{p_o}\right]\frac{1}{p_o^2}(k_i b)^4 + \cdots$$

$$C_2 = \frac{-1}{2m_o p_o}\left(p_2 + \frac{m_2}{2}\right)(k_i b)^2 - \frac{1}{8m_o p_o}\left[\left(p_4 - \frac{m_4}{6}\right)\right.$$
$$\left. + \left(\frac{m_2}{3m_o} - \frac{p_2}{p_o}\right)\left(p_2 + \frac{m_2}{2}\right)\right](k_i b)^4 + \cdots$$

$$C_4 = \frac{1}{192 m_o p_o}\left[\left(3p_4 - \frac{7m_4}{4}\right)\right.$$
$$\left. -2\left(p_2 + \frac{m_2}{2}\right)\frac{m_2}{m_o}\right](k_i b)^4 + \cdots \quad \text{(A2)}$$

where

$$p_\mu = p + M^{\mu/2+1}p' \quad \text{(A3)}$$

$$m_\mu = 1 + M^{\mu/2+1} \quad \text{(A4)}$$

$$M = \frac{n_t^2}{n_i^2} \quad \text{(A5)}$$

$$p = \ln(\gamma) + \ln\left(\frac{k_i b}{4}\right) - \frac{i\pi}{2} \quad \text{(A6)}$$

and

$$p' = p + \ln(\sqrt{M}). \quad \text{(A7)}$$

B. Electric Field Polarized Parallel to the Aperture

We now consider the case where the incident electric field is x-polarized. The relative aperture field is then given by

$$\frac{E_{ap}^x(y, z = 0)}{E_i(y, z = 0)} = k_i b \sum_{j=1}^{\infty} D_j \sin(jv) \quad \text{(A8)}$$

where D_j are expansion coefficients and, once again, $\cos(v) = y/b$. The first three nonzero expansion coefficients of this

geometry are

$$D_1 = -i + \frac{i}{8}\left[r_2 - \frac{3s_2}{4}\right](k_i b)^2$$
$$-\frac{i}{64}\left[\frac{r_4}{2} - \frac{7s_4}{24} + r_2^2 - \frac{3s_2 r_2}{2} + \frac{7s_2^2}{12}\right](k_i b)^4 + \cdots$$

$$D_3 = \frac{i s_2}{96}(k_i b)^2$$
$$-\frac{i}{768}\left[r_4 - \frac{s_4}{8} + s_2 r_2 - \frac{7s_2}{8}\right](k_i b)^4 + \cdots$$

$$D_5 = -\frac{i}{13\,440}[s_4 + s_2^2](k_i b)^4 + \cdots \quad \text{(A9)}$$

where

$$r_\mu = p + M^{\mu/2}p \quad \text{(A10)}$$

and

$$s_\mu = 1 + M^{\mu/2}. \quad \text{(A11)}$$

REFERENCES

[1] L. Rayleigh, "On the passage of waves through apertures in plane screens, and allied problems," *Phil. Mag.,* vol. 43, pp. 259–272, 1897.
[2] C. J. Bouwkamp, "Diffraction theory," *Rep. Progr. Phys.,* vol. 17, pp. 35–100, 1954, and references therein.
[3] D. H. Auston, K. P. Cheung, and P. R. Smith, "Picosecond photoconducting Hertzian dipoles," *Appl. Phys. Lett.,* vol. 45, pp. 284–286, 1984.
[4] C. Fattinger and D. Grischkowsky, "Beams of terahertz electromagnetic pulses," in *OSA Proc. Picosecond Electronics and Optoelectronics.* Washington, DC: Opt. Soc. Amer., 1989, vol. 4, pp. 225–231.
[5] P. U. Jepsen and S. R. Keiding, "Radiation patterns from lens-coupled terahertz antennas," *Opt. Lett.,* vol. 20, pp. 807–809, 1995.
[6] P. M. Downey and J. R. Karin, "Hertzian dipole measurements with InP photoconductors," in *Picosecond Electronics and Optoelectronics,* G. A. Mourou, D. M. Bloom, and C.-H. Lee, Eds. Berlin, Germany: Springer-Verlag, 1985, pp. 201–204.
[7] W. Sha, T. B. Norris, J. W. Burm, D. Woodard, and W. J. Schaff, "New coherent detector for terahertz radiation based on excitonic electroabsorption," *Appl. Phys. Lett.,* vol. 61, pp. 1763–1765, 1992.
[8] J. T. Darrow, "Generation and detection of terahertz radiation with large-aperture photoconducting antennas," Ph.D. dissertation, Columbia Univ., 1992, ch. 4.
[9] M. van Exter and D. Grischkowsky, "High-brightness terahertz beams characterized with an ultrafast detector," *Appl. Phys. Lett.,* vol. 55, pp. 337–339, 1989.
[10] A. Nahata, D. H. Auston, T. F. Heinz, and C. Wu, "Coherent detection of freely propagating terahertz radiation by electro-optic sampling," *Appl. Phys. Lett.,* vol. 68, pp. 150–152, 1996.
[11] J. Bromage, S. Radic, G. Agrawal, C. Stroud, P. Fauchet, and R. Sobolewski, "Spatio-temporal shaping of terahertz pulses," *Opt. Lett,* in press.
[12] G. A. Grinberg, "A new method for solving problems related to the diffraction of electromagnetic waves by a plane with an unbounded straight slit," *Zh. Tekn. Fiz.,* vol. 27, pp. 2410–2419, 1957.
[13] J. S. Asvestas and R. E. Kleinman, *Electromagnetic and Acoustic Scattering by Simple Shapes,* J. J. Bowman, T. B. A. Senior, and P. L. E. Uslenghi, Eds. New York: Hemisphere, 1987, pp. 203–206.
[14] K. Houlberg, "Diffraction by a narrow slit in the interface between two different media," *Can. J. Phys.,* vol. 45, pp. 57–81, 1967.
[15] D. Grischkowsky, S. Keiding, M. van Exter, and Ch. Fattinger, "Far-infrared time-domain spectroscopy with terahertz beams of dielectrics and semiconductors," *J. Opt. Soc. Amer. B,* vol. 7, pp. 2006–2015, 1990.

[16] C. Wu, K. Beeson, P. Ferm, C. Knapp, M. McFarland, A. Nahata, J. Shan, and J.T. Yardley, "High glass transition temperature electro-optic polymers," in *Mater. Res. Soc. Symp. Proc.,* 1994, vol. 328, pp. 477–484.

[17] J. A. Valdmanis and G. Mourou, "Subpicosecond electrooptic sampling: Principles and applications," *IEEE J. Quantum Electron.,* vol. QE-22, pp. 69–78, 1986.

[18] M. van Exter, Ch. Fattinger, and D. Grischkowsky, "Terahertz time-domain spectroscopy of water vapor," *Opt. Lett.,* vol. 14, pp. 1128–1130, 1989.

[19] R. F. Millar, "A note on diffraction by an infinite slit," *Can. J. Phys.,* vol. 38, pp. 38–47, 1960.

[20] C. M. Butler and D. R. Wilton, "General analysis of narrow strips and slots," *IEEE Trans. Antennas Propagat.,* vol. 28, pp. 42–48, 1980.

[21] C. M. Butler, "General analysis of a narrow slot in a conducting screen between half-spaces of different electromagnetic properties," *Radio Sci.,* vol. 22, pp. 1149–1154, 1987.

Ajay Nahata was born in Vadodara, India, on December 31, 1963. He received the B.S. degree from the Massachusetts Institute of Technology, Cambridge, MA, in 1985 and the M.S. degree from Columbia University, New York, NY, in 1987, both in electrical engineering, and is currently pursuing the Ph.D. degree in electrical engineering.

From 1987 to 1992, he was with Allied Signal, Inc., Morristown, NJ. There he studied the nonlinear optical properties of organic materials and their application to integrated optical devices. His current research involves the generation and detection of electromagnetic transients using ultrashort optical pulses.

Mr. Nahata is a member of the Optical Society of America.

Tony F. Heinz was born in Palo Alto, CA, on April 30, 1956. He received the B.S. degree in physics from Stanford University, Palo Alto, CA, in 1978 and the Ph.D. degree in physics from the University of California at Berkeley in 1982.

While at Berkeley, he received support from fellowships of the NSF and of the IBM Corporation. From 1983 until 1995, he was employed at the IBM T. J. Watson Research Center in Yorktown Heights, NY. In 1995, he joined Columbia University, New York, NY, as Professor of Electrical Engineering and Physics. His research interests lie in the areas of ultrafast spectroscopy and nonlinear optics, particularly as applied to surface problems.

Dr. Heinz was awarded the 1995 Prize of the International Commission for Optics in recognition of his contributions to the development and application of optical techniques for the study of surfaces and interface. He is a Fellow of the Optical Society of America and of the American Physical Society and is presently serving as the Editor of the *Journal of the Optical Society of America B.*